Preparation and characterization of free-standing pure porphyrin nanoparticles

ARUN KUMAR PEREPOGU[a] and PRAKRITI RANJAN BANGAL*[b]

[a]Organic Chemistry Division-II, [b]Inorganic and Physical Chemistry Division,
Indian Institute of Chemical Technology, Uppal Road, Tarnaka, Hyderabad, 500 007
e-mail: prakriti@iict.res.in

Abstract. Preparation and characterization of absolutely pure and stable nanoparticles of 5,10,15,20-meso-tetrakis phenyl porphyrin (TPP) and catalytically repute 5,10,15,20-meso-tetrakis pentaflurophenyl porphyrin (H_2F_{20}TPP) by improved 'reprecipitation method' is described. The innovation of this modified 'reprecipitation method' lies on the judicial selection of organic solvent and amount of porphyrin solution to be injected in the aqueous media. Exactly similar process produces relatively small nanoparticles for TPP than that of H_2F_{20}TPP while the stability of the H_2F_{20}TPP nanoparticles is bit higher than nanoparticles of TPP. Absorption and emission spectra reveal that the formation of nanoparticles for both the cases is induced by J- and H-type aggregation. DFT calculations predict the optimized geometries and frontier molecular orbital, which favours the strength of face-to-face interaction with neighbour molecules to be more facile for TPP than that of H_2F_{20}TPP helping the latter to form bigger and relatively more stable and free-standing nanoparticles. The use of no other compounds except dichloromethane, a highly volatile organic solvent and respective porphyrins give absolutely pure nanoparticles. This improved method will lead to produce organic nanoparticles of π-conjugated systems easily and efficiently.

Keywords. Nanoparticles; tetrakis-pentaflurophenylporphyrin; tetrakis-phenylporphyrin; reprecipitation method.

1. Introduction

The recent progress in nanoscience and nanotechnology is mainly due to the ability to synthesize, investigate and exploit materials with structural modulation in nanometer scale. Nanoparticles and/or nanocrystals in semiconductors and metals have been extensively investigated and continuously being investigated from the view point of both science and industry, e.g. thermodynamics, crystal structures, optical properties and reactivity as catalysis.[1,2] The fabrication of the inorganic nanoparticles is generally done either by deposition methods in a molten glass matrix or by vacuum-evaporation and these processes are well developed. But these processes can not be applied conveniently for thermodynamically unstable organic compounds. Hence, preparation and characterization of stable organic nanoparticles of organic compounds of low molecular weight have not yet drawn much attention and example of organic nano-

particles are not many. Thus, effort to prepare stable and free-standing pure organic nanoparticles is indispensable.

However, history of organic nanoparticles/crystals is not extensive unlike inorganic, metallic or semiconductor nanoparticle. Organic nanoparticles are of interest not only because they represent an intermediate situation between single molecules and bulk materials, representing a multichromophoric system but also they offer potential applications in science and technology.[3] In addition, the availability of diverse organic molecules and flexibility in materials synthesis open the door for organic nanoparticles research.[4] Since the discovery of 'reprecipitation method', a 'bottom up' route to synthesize the organic nanoparticle by Kasai *et al*[5] different types of innovative results are being reported playing around the process.[6–18] The central idea of this process is the delicate mixture of good solvent and poor solvent of the target compound. A small volume of milli molar solution of target compound made of relatively volatile solvent is rapidly injected into large amount of vigor-

ously stirred poor solvent of target compound. The good solvent of target compound is miscible with poor solvent of the target compound. Hence, the good solvent is mixed with poor solvent and target compound reprecipitated as nanoparticles or crystals. In general, the good solvent referred to alcohol, acetone and or other organic solvents owing lower boiling point and poor solvent is water. On tuning this process for varieties of good solvent and poor solvent pairs along with different parameters, such as temperature, use of microwave and sonication for different π conjugated systems brings several frantic results, which are documented elsewhere.[6–18]

Xianchang Gong *et al* have claimed that they have first synthesized and characterized the porphyrin nanoparticles using mixing solvent technique.[19] In addition, they have discovered poly ethylene glycol as a stabilizer of the porphyrin nanoparticle. In the process they have chosen the good solvent either DMSO or pyridine and poor solvent as water. However, the DMSO or pyridine cannot be a good solvent for preparing pure organic nanoparticles by 'reprecipitation' method because they are highly non-volatile. It is true, porphyrin is desolved in both DMSO and pyridine and both the solvents are easily misicible in water but these solvents are having boiling point with 189° and 115°C respectively. Furthermore, those solvents easily form moderately strong hydrogen bonding with porphyrin molecules irrespective of hydrogen bonding with water. Hence, removal of the good solvent from poor solvent is highly unlikely even through the boiling of poor solvent (water). As a result, presumed nanoparticles formed in this method is not pure porphyrin nanoparticles rather it is a nanoparticle of porphyrin-DMSO or porphyrin-pyridine cluster. Formation of hydrogen bonding of porphyrin with DMSO or pyridine does not change the photophysical properties (absorption and fluorescence) of porphyrin except little decrease in absorbance in Soret band. Furthermore, they have used poly ethylene glycol (PEG) as stabilizer for porphyrin nanoparticle, which could make hydrogen bonding complex with pyrrole N-atom in porphyrin macrocycle leading to give nanocomposite of porphyrin/DMSO/PEG or porphyrin/pyridine/PEG, rather than only pure porphyrin nanoparticles. Indeed, references to the production of pure porphyrin nanoparticles are remarkably sparse in view of the few available literature on the subject. To further advance the situation, we present here the most simple and tuned process to prepare absolutely pure and discrete free-standing nanoparticle

of catalytically repute 5,10,15,20, meso-Tetrakis pentafluorophenyl porphyrin ($H_2F_{20}TPP$) and very common 5,10,15,20, meso-Tetrakis phenyl porphyrin (TPP), structures are shown in figure 1, where no other compounds have been used. This process could be implemented for other hydrophobic porphyrin systems and it is under progress.

2. Experimental

2.1 *Synthesis of porphyrin nanoparticles*

5,10,15,20-meso-tetrakis petafluorophenyl porphyrin ($H_2F_{20}TPP$) and 5,10,15,20-meso-tetrakis phenyl porphyrin were purchased from Aldrich Chemical Co. and used without further purification. To prepare nanoparticles we adopted 'reprecipitation method' and it is described elsewhere[5]. In brief, first of all stock solution of said porphyrins of milliMolar concentration were prepared in dichloromethane (DCM) (HPLC grade, Aldrich) and stored in the dark place at room temperature. Then few microliter of stock solution of porphyrin was rapidly injected into large excess of deionized water at room temperature and sonicated for few minutes. A very light yellow colloid was obtained and used for characterization.

2.2 *Characterization of the porphyrin nanoparticles*

Scanning electron microscopy was performed on a Hitachi S-3000N scanning electron microscope operating at 10 kV. The samples for SEM imaging were coated with gold. Transmission micrograph was taken using FEI Tecnai F12 (Philips Electron Optics, Holland), operated at 100 kV. A drop of colloid solution was placed on a carbon coated copper grid and allowed to dry at ambient temperature before recoding
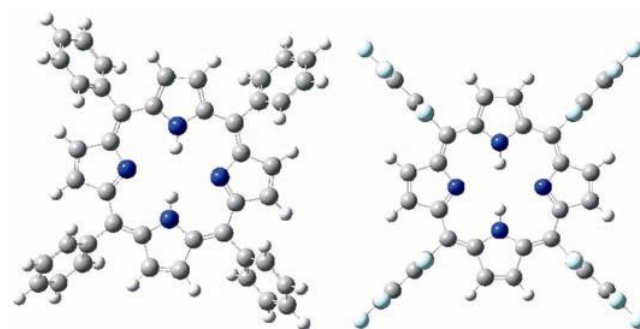

Figure 1. Ground state optimized structure. TPP (left) and H_2F_{20} TPP (right).

the micrograph. UV-visible absorption spectra were obtained with JASCO V-550 UV/VIS spectrophotoeter. The steady-state fluorescence measurements were carried out on a Spex Fluorolog-3 spectrofluorometer. Absorption and emission spectra of nanoparticles were directly taken from the prepared nanoparticles colloid as described above. Due to colloid nature of the nanoparticle solution absorption baseline was increased and baseline correction was made using baseline correction option in Microcal origin software.

3. DFT method

To compare the ground state geometries and frontier molecular orbital of TPP and $H_2F_{20}TPP$ we have performed geometry optimization calculation by density functional method. All computations were performed by using the GAUSSIAN 03/Rev-B.03 package[20] implemented on Intel Pentium-4 PC machines. The optimization of the geometries and population analysis were carried out using the generalized-gradient approximation Becke–Lee–Yang–Parrs BLYPd level of theory with 6-311G basis set. Geometry optimizations were continued up to reaching the normal criteria implemented in GAUSSIAN 03. Molecular drawings were obtained through the Gauss View 03 software package.

4. Results and discussions

In a typical preparation of porphyrin nanoparticles, 30 μl of a 1·0 mM solution of $H_2F_{20}TPP$ or TPP (molecular structures are shown in figure 1) in dichloromethane (DCM) was rapidly injected into 5 mL of deionized water by high precision micro-liter syringe at room temperature under strong sonicated condition. A light yellow transparent colloid-like solution was obtained after sonication for approximately 15 min. Casting a drop of colloidal porphyrin solution directly onto cleaned stub and using scanning electron microscopy (SEM) as well as putting a drop on copper grid and using transmission electron microscope, the colloidal porphyrin particles prepared were observed to be a collection of nanoparticles of ∼ 50–250 nm diameter for $H_2F_{20}TPP$ and ∼ 30–200 nm for TPP (figure 2).

Mechanistically we have selected DCM as good solvent. The solubility ratio of DCM in water is 1 : 100. Due to the fact, injection of 30 μl porphyrin solution in DCM into 5 ml water will not only easily
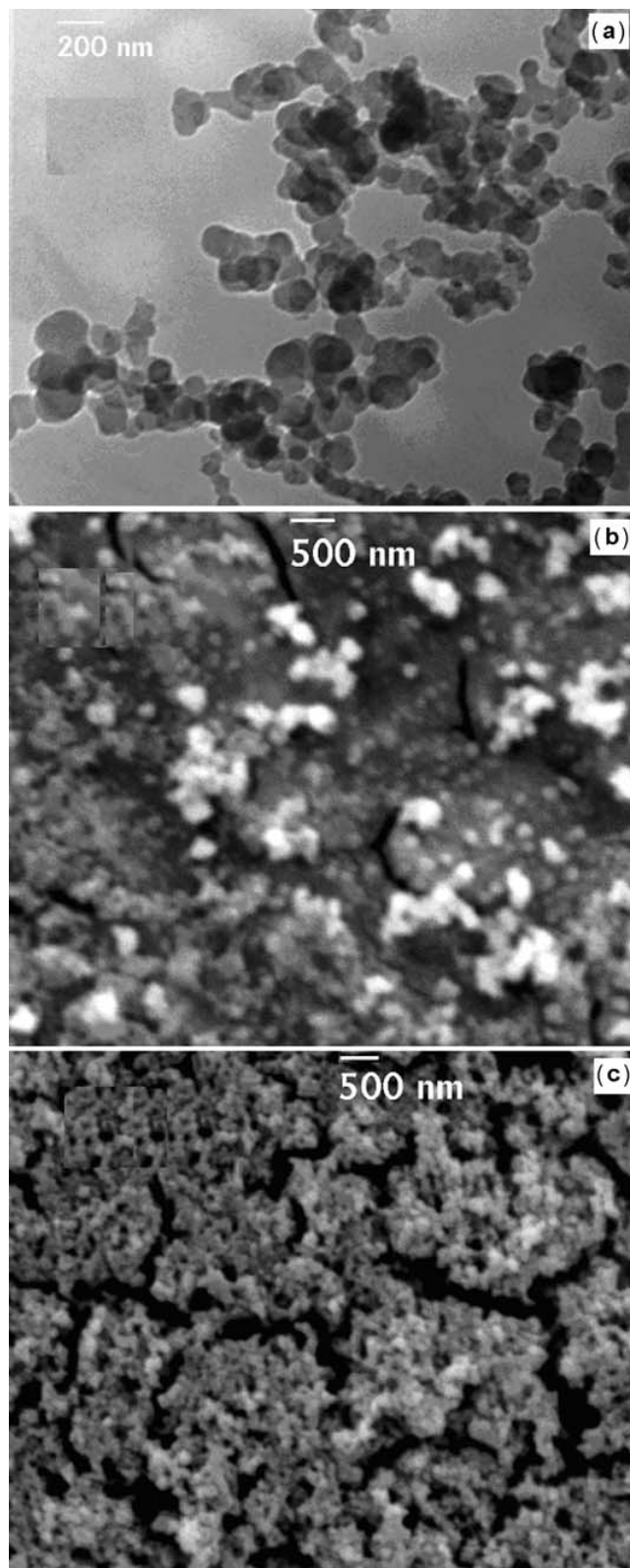

Figure 2. (a) TEM images of $H_2F_{20}TPP$ nanoparticles, (b) SEM Image of $H_2F_{20}TPP$ and (c) SEM images of TPP nanoparticles onto metallic stub. A drop of colloid solution of nanoparticles was deposited onto stub and dried under ambient temperature before deposition of gold coating for recoding micrograph by SEM.
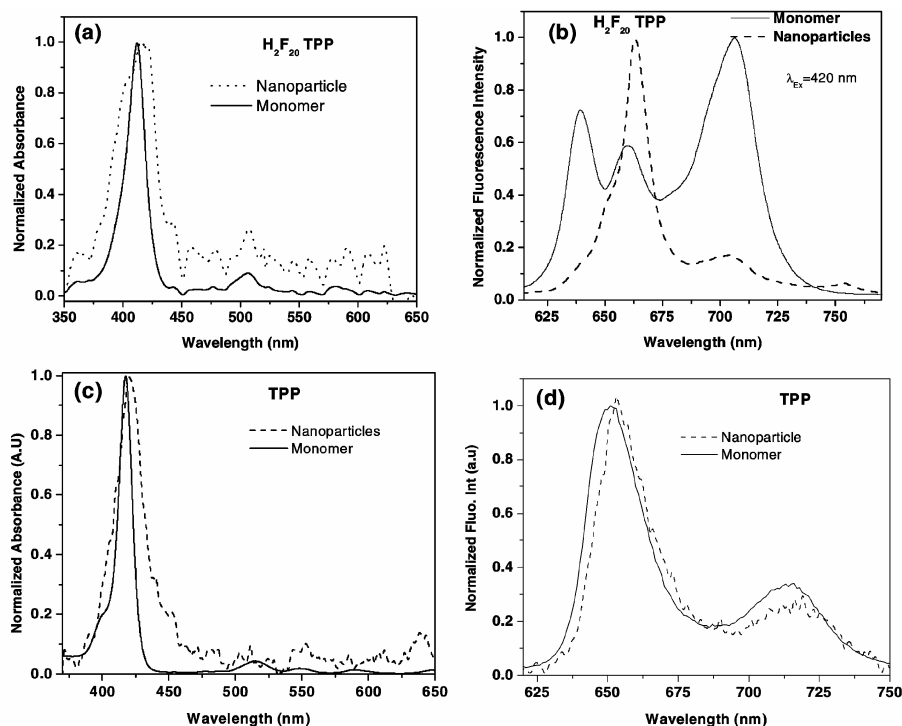
Figure 3. (**a**) Normalized absorption spectra of $H_2F_{20}TPP$ monomer in DCM and nanoparticles in water, (**b**) Normalized fluorescence spectra of $H_2F_{20}TPP$ monomer in DCM and nanoparticles in water, (**c**) Normalized absorption spectra of TPP monomer in DCM and nanoparticles in water, (**d**) Normalized fluorescence spectra of TPP monomer in DCM and nanoparticles in water.

be mixed with water but also will be evaporated very fast and porphyrin will be reprecipitated as nanoparticle/crystal in water producing colloid solution of nanoparticles. The colloid solution produced by this method was found to be much stable and it was observed to sustain more than 90 days for $H_2F_{20}TPP$ and 45 days for TPP replicating the SEM image as well as producing no precipitation. DCM being highly volatile it could be evaporated easily even after being mixed with water leaving the produced nanoparticles dispersed in pure aqueous medium and this might have led to improve the stability of the nanoparticles.

Figure 3a portraits the Uv-vis absorption spectra of $H_2F_{20}TPP$ monomer in DCM solvent and its nanoparticles in water. Not surprisingly, the Soret band of nanoparticles is found to be composed of two extra absorption peaks at 403 and 420 nm around the monomer absorption peak at 412 nm indicating the existence of both J-type and H-type aggregates along with monomer in almost equal proportion. The fluorescence spectra of $H_2F_{20}TPP$ monomer in DCM and corresponding nanoparticles in water are shown in figure 3b when excited at 420 nm. The fluores-

cence emission spectra of the nanoparticles of $H_2F_{20}TPP$ show strong and narrow band at 663 nm along with weak emission peaks for residual monomer at 630 and 703 nm. In addition, a weak peak at 754 nm is observed. The fluorescence intensity increases 1·5 times than that of monomer. The dominating fluorescence peak of $H_2F_{20}TPP$ nanoparticles at 663 nm is assigned to be the emission from J-aggregate and the new peak at 754 nm could be due to secondary splitting arising from the end-to-end interaction between two J-aggregates. The UV-vis spectra of TPP nanoparticles along with TPP monomer are presented in figure 3c. Close inspection reveals that the Soret band of TPP nanoparticles is composed of two extra peaks at 410 and 420 nm along with the monomer absorption peak at 417 nm confirming the existence of both H- and J-type aggregate. The fluorescence emission spectra of TPP nanoparticles are red shifted by 3 nm and become narrower than that of monomer (figure 3d) and fluorescent intensity increases 2·5 times than that of monomer.

In general, porphyrins easily form aggregate through hydrophobic interaction and π–π stacking with adjacent molecules.[21–33] Peripheral substitutions on por-
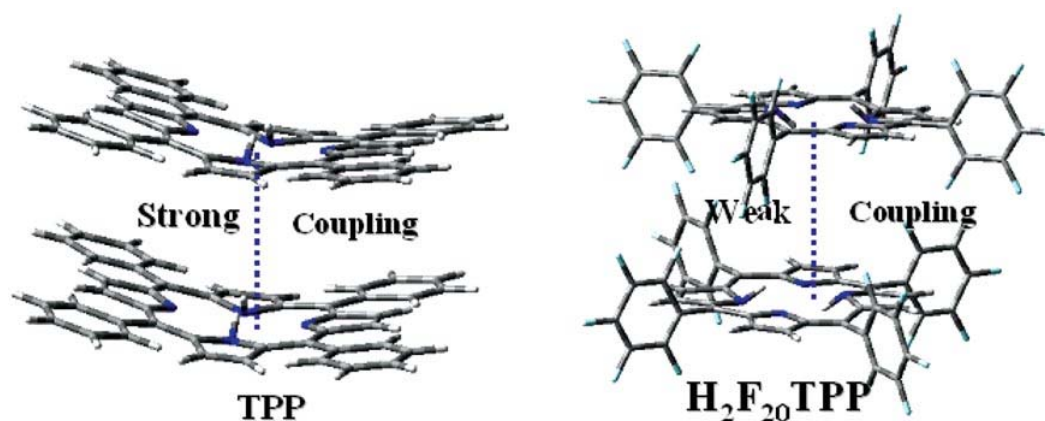
Figure 4. Schematic approach for possible aggregate formation for TPP and $H_2F_{20}TPP$.

phyrin could lead to changing the strength of inter-molecular interactions and to control the size and structures of aggregated form. DFT calculations with 6-311G basis set clearly reveal that ground state optimization structure of $H_2F_{20}TPP$ strongly differs from the ground state optimized structure of TPP (figure 1). Pentaflurophenyl group of $H_2F_{20}TPP$ lies exactly in orthogonal direction (out-of–plane of porphyrin macrocycle) with respect to porphyrin macrocycle, where as phenyl ring of TPP maintains out-of-plane of porphyrin macrocycle with lower tilt angle. This result suggests that the $\pi-\pi$ stacking with adjacent molecules for $H_2F_{20}TPP$ is geometrically less favoured than TPP. Different models for dimer formation could be proposed for both the molecules describing the inter-planer distances. A representative schematic illustration of TPP-TPP and $H_2F_{20}TPP$-$H_2F_{20}TPP$ approach to form respective dimer is shown in figure 4. In case of TPP dimer, the constituent monomers tend to be more planer resulting facile $\pi-\pi$ interaction between the monomers and a distant between two monomers is calculated to be ~5·5 Å whereas, for $H_2F_{20}TPP$ dimmer the structure of the constituent monomers remains same resulting weak $\pi-\pi$ interaction between two monomers and a distance between two monomers is calculated to be 8·2 Å. Frontier MO calculations show that HOMO and HOMO-1 are nearly degenerate where as LUMO and LUMO-1 are strictly degenerate for both the porphyrins. The four orbital model proposed by Gouterman[34] is well accepted model to interpret the electronic absorption spectra of porphyrin compounds, where it assumed that the HOMO and HOMO-1 of a porphyrin molecule are nearly degenerate while the LUMO and LUMO-1 are rigorously degenerate. Our

calculations fully support the four orbital model of Gouterman. The HOMO, HOMO-1, LUMO and LUMO-1 orbital surface are depicted with corresponding energy in figure 5. These frontier molecular orbital (FMO) clearly shows that HOMO and LUMO of TPP are delocalized not only on the porphyrin macrocyle but also on the peripherial phenyl ring, where as HOMO and LUMO are fully localized only on the porphyrin macrocycle in $H_2F_{20}TPP$ (figure 5). This result suggests that $\pi-\pi$ stacking to the adjacent molecules is relatively less extensive in $H_2F_{20}TPP$ than TPP. Furthermore, sequential substitution of pentafluorophenyl group in place of phenyl in 5,10,15,20 meso-Tetrakis phenyl porphyrin (TPP) clearly shows the trend of decrease of HOMO and LUMO energies making it soft electron acceptor. Calculation shows that the HOMO and LUMO energies of $H_2F_{20}TPP$ are –6·21 and –3·35 eV where as for TPP these values are –4·9 eV and –2·25 eV, respectively. Considering the molecular orbital theory approaches, it could be inferred that $H_2F_{20}TPP$ is more electronegative than TPP, when the HOMO energy (ε_{HOMO}) is related to the ionization potential (IP) by Koopmanns' theorem and the LUMO energy (ε_{LUMO}) is used to estimate the electron affinity (EA). If $\varepsilon_{HOMO} \approx$ IP and $\varepsilon_{LUMO} \approx$ EA, then the average value of the HOMO and LUMO energies is related to the electronegativity (χ) defined by Mulliken[35] as $\chi = (IP + EA)/2$ and according to the definition the χ values of $H_2F_{20}TPP$ and TPP are about –4·78 and –3·58 eV respectively. However, due to these factors, the $\pi-\pi$ interactions between $H_2F_{20}TPP$ molecules could be weaker than that of TPP molecules and it leads to produce bigger nanoparticles for $H_2F_{20}TPP$. Similarly, the tendency of the formation
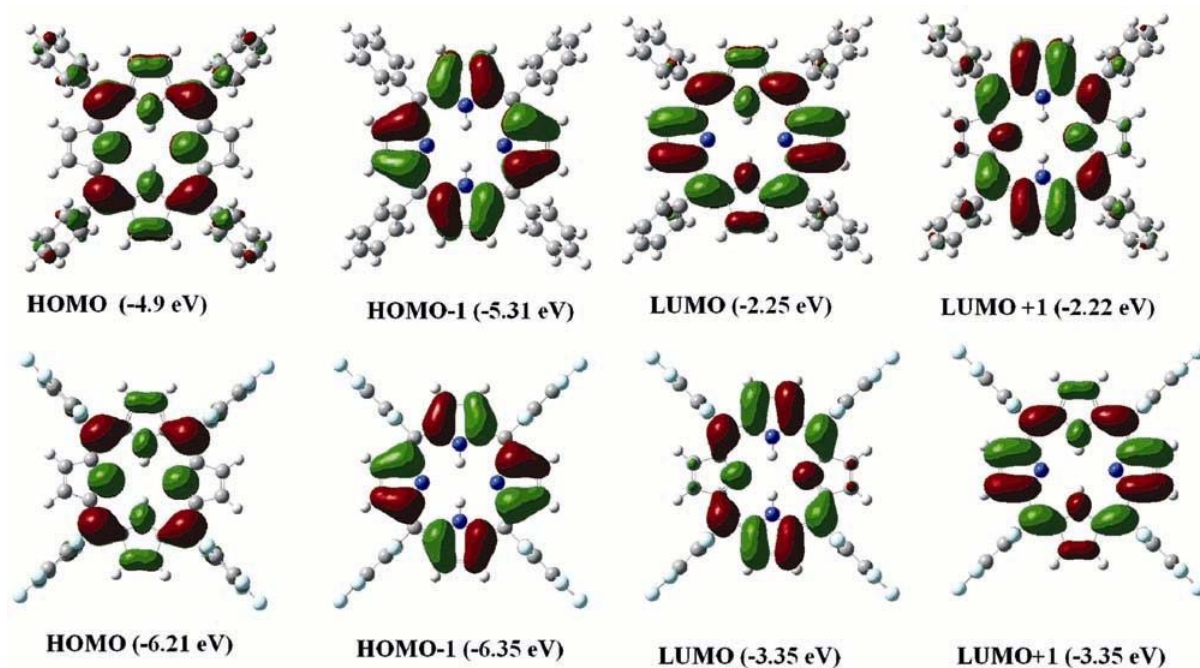
Figure 5. Calculated orbital energy (in parenthesis) and surface (0.02 eau^{-3}) plot of frontier HOMO, HOMO-1 and LUMO, LUMO + 1 of TPP (top panel) and H_2F_{20} TPP (bottom panel). Within a given orbital the two colours correspond to positive and negative phases of the wave function respectively.

of face-to-face or tail-to-tail geometries for H_2F_{20}TPP through $\pi–\pi$ interaction is also diminished and the formed colloid of H_2F_{20}TPP nanoparticles become more stable than the colloid of TPP nanoparticles (supporting info). In addition, due to strong volatility of DCM, it evaporates from water within short time and nanoparticles are dispersed strictly in aqueous phase increasing the stability of nanoparticles for quite long period.

5. Conclusion

In conclusion, we demonstrate a simple and convenient method for preparation of absolutely pure and stable H_2F_{20}TPP and TPP nanoparticles with ~ 50–250 nm and 30–200 nm diameter respectively. The uniqueness of this method is judicial selection of organic solvent as well as simplicity, a demanding merit of 'reprecipitation method'. The possibility of tuning the size and photophysical properties of the nanoparticles using this process on changing the substituents on the porphyrins or introduction of the metal ions inside the macrocycle along with judicial selection of other organic solvents will open the way to synthesize not only verities of porphyrin nanoparticles but also other organic nanoparticles with potential applications and this is under progress. At-

tempts are also underway to understand the differences and similarities in the photo-physical and photo-chemical properties of the nanoparticles and monomers in terms of the application of these porphyrin nanoparticles in dye sensitized opto-electronic devices as well as triplet sensitizer.

Supporting information: Additional SEM images taken at different ages of nanoparticles.

References

1. Hulst H C van der 1981 in *Light scattering by small particles* (New York: Dover Publications Inc.)
2. Murray C B, Norris D J and Bawendi M G 1993 *J. Am. Chem. Soc.* **115** 8706
3. Masuhara H and Kawata S 2004 in *Nanophotonics* (New York: Elsevier) vol 1
4. Masuhara H, Nakanishi H and Sasaki K 2003 in *Single organic nanoparticles* (Heidelberg: Springer)

5. Kasai H, Nalwa H S, Oikawa H, Okada S, Matsuda H, Minami N, Kakuta A, Ono K, Mukoh A and Nakanishi H 1992 *Jpn. J. Appl. Phys. Part 2* **31** L1132

6. Kasai H, Kamatani H, Yoshikawa Y, Okada S, Oikawa H, Watanabe A, Ito O and Nakanishi H 1997 *Chem. Lett.* 1181

7. Ai-Dong Peng, De-Bao Xaio, Ying Ma, Wen Sheng and Jain-Nain Yao 2005 *Adv. Mater.* **17** 2070

8. Drain C M, Smeureanu G, Patel S, Gong X, Garno J and Arijeloye J 2006 *New J. Chem.* **30** 1834

9. Sun W O and Young S K 2005 *Colloids and Surfaces A: Physicochemical and Engineering Aspects* **415** 257–258

10. Takahashi Y, Kasai H, Nakanishi H and Suzuki T M 2006 *Angew Chem. Int. Ed.* **45** 913

11. Gesquiere A J, Uwada T, Asahi T, Masuhara H and Barbara Paul F 2005 *Nano Lett.* **5** 1321

12. Kim H Y, Bjorklund T G, Lim S-H and Bardeen C J 2003 *Langmuir.* **19** 3941

13. Jin-Song Hu, Yu-Guo Guo, Han-Pu Liang, Li-Jun Wan and Li Jiang 2005 *J. Am. Chem. Soc.* **127** 17090

14. Zhang X, Zhang Xiaohong, Zou Kai, Lee Chun-Sing and Lee Shuit-Tong 2007 *J. Am. Chem. Soc.* **129** 3527

15. Fu H B and Yao J N 2001 *J. Am. Chem. Soc.* **123** 1434

16. Al-Kaysi R O, Muller A M, Ahn Tai-Sang, Lee S and Bardeen C J 2005 *Langmuir.* **21** 7990

17. Shayu Li, Liming He, Fei Xiong, Yi Li and Guoqiang Y 2004 *J. Phys. Chem.* **B108** 10887

18. Wang X, Li Z, Medforth C J and Shelnutt J A 2007 *J. Am. Chem. Soc.* **129** 2440

19. Gong X, Milic T, Xu C, Batteas J D and Drain C M 2002 *J. Am. Chem. Soc.* **124** 14290

20. Gaussian 03, Revision-B.03, Gaussian, Inc., Pittsburgh PA, 2003

21. Li L L, Yang C J, Chen W H and Lin K J 2003 *Angew. Chem. Ind. Ed.* **42** 1505

22. Lin K J 1999 *Angew. Chem. Ind. Ed.* **38** 2730

23. Diskin-Posner Y, Dahal S and Golberg I 2000 *Angew. Chem. Ind. Ed.* **39** 1288

24. Li G, Fudickar W, Skupin M, Klyszcz A, Draeger C, Lauer M and Fuhrhop J H 2002 *Angew. Chem. Ind. Ed.* **41** 1828

25. De Schryver F C, Rowan A E and Nolte R J 1999 *Langmuir.* **15** 3582

26. Koti A S and Periasamy R N 2002 *J. Mater. Chem.* **12** 2312

27. van der Boom T, Hayes R T, Zahao Y, Bushard P J, Weiss E A and Wasielewski M R 2002 *J. Am. Chem. Soc.* **124** 9582

28. Tsuda A, Sakamoto S, Yamaguchi K and Aida T 2003 *J. Am. Chem. Soc.* **125** 15722

29. Balaban T S, Goddard R, Linke-Schaetzel M and Leng J M 2003 *J. Am. Chem. Soc.* **125** 4233

30. Takahashi R and Kobuke Y J 2003 *J. Am. Chem. Soc.* **125** 2372

31. Kuroda Y, Sugou K and Sasaki K 2000 *J. Am. Chem. Soc.* **122** 7833

32. Koti A S R and Periasamy N 2002 *J. Mater. Chem.* **12** 2312

33. Doon S C, Shanmughan S, Aston D E and Mettal J L 2005 *J. Am. Chem. Soc.* **127** 5885

34. Gouterman M 1961 *J. Mol. Spectrosc.* **6** 138

35. Mulliken R S 1934 *J. Chem. Phys.* **2** 782